



# Optics Letters

## Control of orbital angular momentum with partially coherent vortex beams

YONGTAO ZHANG,<sup>1,2</sup>  YANGJIAN CAI,<sup>3,4</sup> AND GREG GBUR<sup>2,\*</sup> 

<sup>1</sup>College of Physics and Electronic Information & Henan Key Laboratory of Electromagnetic Transformation and Detection, Luoyang Normal University, Luoyang 471934, China

<sup>2</sup>Department of Physics and Optical Science, University of North Carolina at Charlotte, Charlotte, North Carolina 28277, USA

<sup>3</sup>Shandong Provincial Engineering and Technical Center of Light Manipulations & Shandong Provincial Key Laboratory of Optics and Photonic Device, School of Physics and Electronics, Shandong Normal University, Jinan 250014, China

<sup>4</sup>School of Physical Science and Technology, Soochow University, Suzhou 215006, China

\*Corresponding author: gjgbur@uncc.edu

Received 5 April 2019; revised 6 June 2019; accepted 6 June 2019; posted 20 June 2019 (Doc. ID 364414); published 17 July 2019

**We investigate the orbital angular momentum of partially coherent beams which are constructed by a superposition of mutually incoherent vortex modes, each mode having a different beam width and topological charge. It is shown that these simple beams nevertheless provide great flexibility in controlling orbital angular momentum through adjustment of the beam parameters and have significant potential for particle rotation and trapping.** © 2019 Optical Society of America

<https://doi.org/10.1364/OL.44.003617>

During the past few decades, there has been a growing interest in singular optics, the study of singularities in optical wave fields, originating with the pioneering work of Nye and Berry [1–4]. Notably in 1992, Allen *et al.* demonstrated that Laguerre–Gaussian beams, possessing a phase vortex core, consequently carry a well-defined orbital angular momentum (OAM) [5]. Since then, OAM has become an important aspect of singular optics, due to its use in applications such as optical tweezers [6], optical spanners [7], and free-space information transfer [8].

The field of singular optics, which has traditionally focused on monochromatic light, has been extended to the study of fields with spatial and temporal fluctuations. Such partially coherent beams have some unique characteristics and advantages in practical applications, such as free-space optical communication [9], particle trapping [10], and atom cooling [11]. Unlike spatially coherent beams, however, partially coherent beams do not have a well-defined phase, and consequently do not typically possess optical phase vortices. In 2003, though, Schouten *et al.* demonstrated that the complex correlation functions of partially coherent fields possess analogous singularities [12], and since then much attention has been given to the vortices of correlation functions [13–17]. Several investigations have concentrated on studying OAM for partially coherent beams [18–20] and the unique characteristics of OAM in such beams. Recently, it was found that three fundamental

classes of partially coherent vortex beams can be distinguished by the different distributions of OAM in their cross-sections, representing Rankine vortices, rigid body rotators, and fluid rotators. These results suggest that partially coherent beams can provide greater control over OAM than their fully coherent counterparts [21].

In this Letter, we investigate how much control over OAM one has in a partially coherent beam by considering beams that are constructed as an incoherent superposition of vortex modes, each mode having a different beam width and topological charge. The construction of a partially coherent vortex beam by such a superposition was introduced in Refs. [21,22], and its OAM properties were discussed in [21]. Each mode in the beams of [21,22] had the same topological charge, however, and those beams are a special case of the partially coherent vortex beams we study here. Our results show that even a small number of modes provide great flexibility in controlling OAM through variation of the beam parameters, including control over the radial distribution of OAM; these results show great potential for particle rotation and trapping, and the development of light-powered micromachines.

For this Letter, we consider a very simple class of partially coherent beams, which may be written as the incoherent superposition of a finite number of different Laguerre–Gauss field modes of radial order  $n_\alpha$  and azimuthal order  $m_\alpha$ , for which the cross-spectral density may be written in the form

$$W(\mathbf{r}_1, \mathbf{r}_2, z) = \sum_{\alpha=1}^N \lambda_\alpha U_{n_\alpha m_\alpha}^*(\mathbf{r}_1, z) U_{n_\alpha m_\alpha}(\mathbf{r}_2, z), \quad (1)$$

where  $\lambda_\alpha \geq 0$  are non-negative weights and  $U_{n_\alpha m_\alpha}(\mathbf{r}, z)$  are the normalized Laguerre–Gauss modes. To produce nontrivial OAM states, we consider modes with different widths in the beam waist. The modes are therefore mutually incoherent, as there are no interference terms in our representation, but not generally orthogonal. This can be readily achieved, for example, by simply superimposing beams from independent laser sources. Equation (1) differs from the venerable coherent mode

representation [23] in that the modes are not part of an orthonormal basis set.

Each Laguerre–Gauss mode can be expressed as [4]

$$U_{n_\alpha m_\alpha}(\mathbf{r}, z) = C_\alpha(z) L_{n_\alpha}^{|m_\alpha|} \left[ \frac{2r^2}{w_\alpha^2(z)} \right] r^{|m_\alpha|} \exp \left[ -r^2 \left( \frac{1}{w_\alpha^2(z)} + \frac{ik}{2R_\alpha(z)} \right) \right] \times \exp(im_\alpha\varphi) \exp[-i\Phi_\alpha(z)(2n_\alpha + |m_\alpha| + 1)], \quad (2)$$

with

$$C_\alpha(z) = \sqrt{\frac{2n_\alpha!}{\pi w_\alpha^2(z)(n_\alpha + |m_\alpha|)!}} \left( \frac{\sqrt{2}}{w_\alpha(z)} \right)^{|m_\alpha|}, \quad (3)$$

$$w_\alpha(z) = w_\alpha \sqrt{1 + z^2/z_\alpha^2}, \quad R_\alpha(z) = z + z_\alpha^2/z, \quad (4)$$

$$\Phi_\alpha(z) = \arctan(z/z_\alpha), \quad z_\alpha = \pi w_\alpha^2/\lambda, \quad (5)$$

where  $w_\alpha(z)$  and  $w_\alpha$  are the beam widths of each Laguerre–Gauss mode at the propagation distances  $z$  and  $z = 0$ , respectively.  $L_{n_\alpha}^{|m_\alpha|}$  is an associated Laguerre function of order  $n_\alpha$  and  $m_\alpha$ , and  $\varphi$  is the azimuthal angle.  $R_\alpha(z)$  is the radius of the wavefront curvature,  $\Phi_\alpha(z)$  represents the Gouy phase, and  $z_\alpha$  is the Rayleigh range of each mode.

For a paraxial scalar partially coherent beam, the OAM flux density along the  $z$  axis may be written as [19]

$$M_d(\mathbf{r}, z) = \frac{\epsilon_0}{k} \text{Im}[\partial_{\varphi_2}(W(\mathbf{r}_1, \mathbf{r}_2, z))]_{\mathbf{r}_1=\mathbf{r}_2}. \quad (6)$$

The OAM flux density depends on the intensity of the beam as well as its transverse spatial distribution. To better understand the physics of the OAM distribution, we define the normalized OAM flux density

$$m_d(\mathbf{r}, z) = \frac{\hbar\omega M_d(\mathbf{r}, z)}{S(\mathbf{r}, z)}, \quad (7)$$

where  $S(\mathbf{r}, z)$  is the  $z$  component of the Poynting vector, which is of the form

$$S(\mathbf{r}, z) = \frac{k}{\mu_0\omega} W(\mathbf{r}, \mathbf{r}, z). \quad (8)$$

The quantity  $m_d$  represents the average OAM flux density per photon, and it is independent of any effects due to the beam envelope. In Ref. [21], this quantity was used to show that certain fundamental classes of partially coherent OAM beams act like pure rigid-body rotators (with a quadratic OAM dependence), pure fluid-body rotators (with a constant OAM dependence), or a Rankine vortex (quadratic core, constant outskirts). We will refer to the OAM flux density per photon as the “distribution of OAM” for brevity.

On substitution from Eqs. (1) and (2) into Eqs. (6)–(8), we can get the expression for the distribution of OAM for our class of partially coherent vortex beams after a propagation distance  $z$ , i.e.,

$$m_d = \hbar \frac{\sum_{\alpha=1}^N \lambda_\alpha |C_\alpha(z)|^2 \left[ L_{n_\alpha}^{|m_\alpha|} \left( \frac{2r^2}{w_\alpha^2(z)} \right) \right]^2 r^{2|m_\alpha|} \exp \left( -\frac{2r^2}{w_\alpha^2(z)} \right) m_\alpha}{\sum_{\alpha=1}^N \lambda_\alpha |C_\alpha(z)|^2 \left[ L_{n_\alpha}^{|m_\alpha|} \left( \frac{2r^2}{w_\alpha^2(z)} \right) \right]^2 r^{2|m_\alpha|} \exp \left( -\frac{2r^2}{w_\alpha^2(z)} \right)}. \quad (9)$$

Equation (9) shows that the distribution of OAM depends on  $w_\alpha(z)$ ,  $m_\alpha$ ,  $n_\alpha$ ,  $\lambda_\alpha$ ,  $z$ , and  $N$ , which suggests that adjusting

these parameters provides great flexibility in controlling not only the total OAM of the beam but how that OAM is distributed in the beam’s cross-section. If all the modes have the same topological charge  $m$ , Eq. (9) reduces to  $m_d = m\hbar$ , which means that the beam acts like a fluid rotator.

The total average OAM per photon can be given by the ratio of the integrated  $M_d(\mathbf{r}, z)$  and  $S(\mathbf{r}, z)$ :

$$m_t(\mathbf{r}, z) = \frac{\hbar\omega \int M_d(\mathbf{r}, z) d^2r}{\int S(\mathbf{r}, z) d^2r}. \quad (10)$$

With the help of Eqs. (1), (2), (6), and (8), the total average OAM per photon of the partially coherent vortex beam can be expressed as

$$m_t = \hbar \frac{\sum_{\alpha=1}^N \lambda_\alpha m_\alpha}{\sum_{\alpha=1}^N \lambda_\alpha}. \quad (11)$$

It is important to note that the total OAM per photon depends on  $m_\alpha$  and  $\lambda_\alpha$  of each mode, indicating that by adjusting  $m_\alpha$  and  $\lambda_\alpha$  of each mode we can also control the total OAM. Equation (11) reduces to  $m_t = m\hbar$  when all the modes have the same topological charge  $m$ .

To illustrate the possibilities in controlling OAM in partially coherent beams, we reduce our general results to two special cases,  $N = 2$  and  $N = 3$ , and consider how the total OAM and distribution of OAM depend on the beam parameters.

Figure 1 shows how the distribution of OAM can be adjusted within a beam cross-section by adjusting the relative widths of a pair of modes. The total OAM is zero, but the beam has a positive OAM core surrounded by negative OAM outskirts. The size and shape of the core region is readily adjusted by changing the beam widths.

More unusual distributions of OAM can be achieved by varying the azimuthal orders of the constituent beams. In Fig. 2, the distributions are shown for a number of different orders; because the modes are equally weighted, the total OAM is simply the average of the totals of each beam. Here, we can see that it is possible to create multiple counter-rotating regions at different radial distances with an appropriate choice of order and beam widths.

The radial order can also play a significant role in creating new counter-rotating regions. In Fig. 3, examples of distributions for nonzero radial orders are shown. The sharp drops correspond to those points where the first beam has a zero ring of

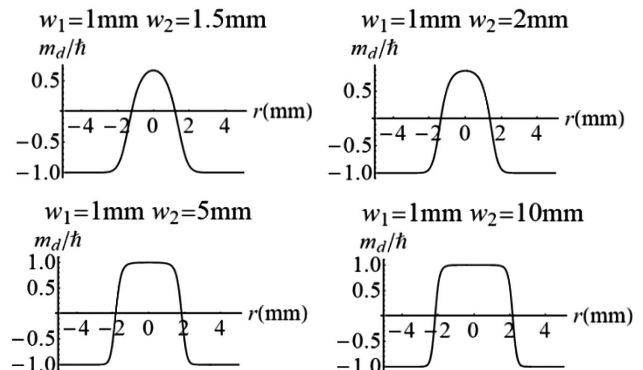


**Fig. 1.** Distributions of normalized OAM flux density  $m_d/\hbar$  at  $z = 0$  with  $m_1 = +1$ ,  $m_2 = -1$ ,  $n_1 = n_2 = 0$ , and  $\lambda_1 = \lambda_2 = 1$ .

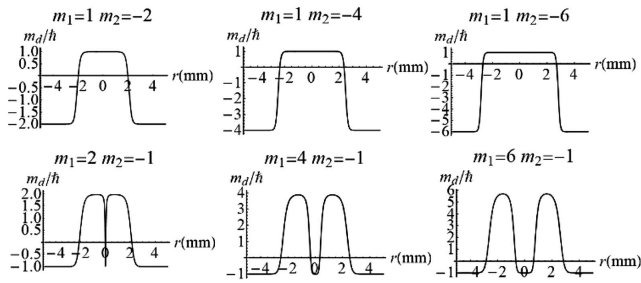


**Fig. 2.** Distributions of normalized OAM flux density  $m_d/h$  at  $z = 0$  with  $w_1 = 1$  mm,  $w_2 = 5$  mm,  $n_1 = n_2 = 0$ , and  $\lambda_1 = \lambda_2 = 1$ .

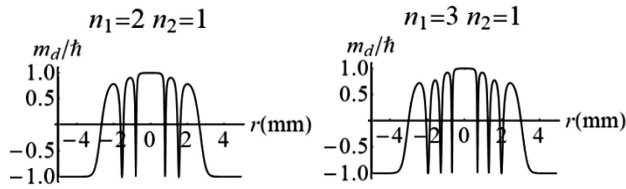


**Fig. 3.** Distributions of normalized OAM flux density  $m_d/h$  at  $z = 0$  with  $w_1 = 1$  mm,  $w_2 = 5$  mm,  $m_1 = +1$ ,  $m_2 = -1$ , and  $\lambda_1 = \lambda_2 = 1$ .

intensity, and the OAM is therefore dominated by the second beam.

These distributions change shape on propagation due to the different spreading characteristics of modes with different widths, but these simple two-mode examples are relatively robust. In Fig. 4, the evolution of the OAM distribution is shown for short propagation distances. It is to be noted that the total OAM remains constant and equal to zero for this case.

Adding additional modes allows us greater and finer control over how OAM is distributed within the beam's cross-section. In Fig. 5, the distribution of OAM in three-mode combinations is illustrated for select choices of beam widths. It is to be noted that the width, depth, and shape of the negative OAM regions can be changed significantly by variation of the beam width.

Even more significant variations can be made by keeping the beam widths constant and changing the azimuthal order of the

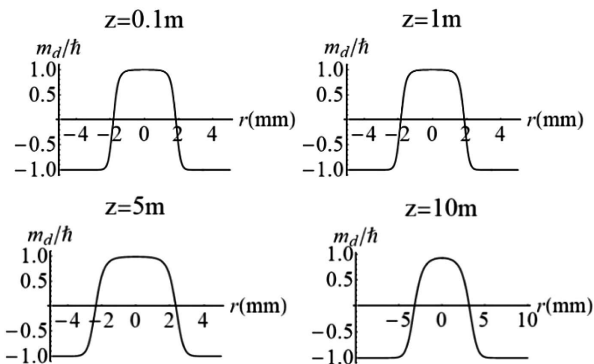


**Fig. 4.** Distributions of normalized OAM flux density  $m_d/h$  with  $w_1 = 1$  mm,  $w_2 = 5$  mm,  $m_1 = +1$ ,  $m_2 = -1$ ,  $n_1 = n_2 = 0$ ,  $\lambda_1 = \lambda_2 = 1$ , and  $\lambda = 632.8$  nm.

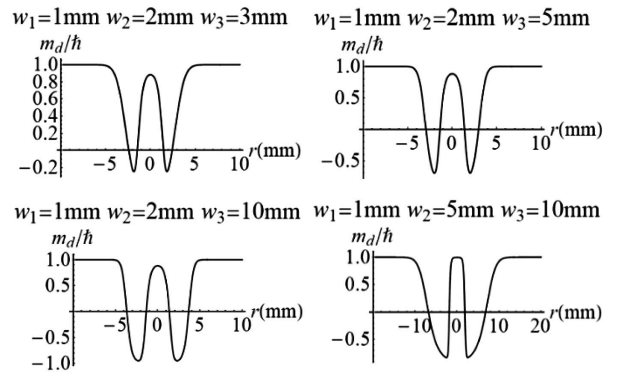


**Fig. 5.** Distributions of normalized OAM flux density  $m_d/h$  at  $z = 0$  with  $m_1 = +1$ ,  $m_2 = -1$ ,  $m_3 = 1$ ,  $n_1 = n_2 = n_3 = 0$ , and  $\lambda_1 = \lambda_2 = \lambda_3 = 1$ .

three modes, as illustrated in Fig. 6. Even with only three modes, it is possible to create multiple regions of positive and negative OAM of different strengths. As seen in Fig. 7, changing the radial order of the beams allows even more variation, and more rapid variation, of the OAM distribution.

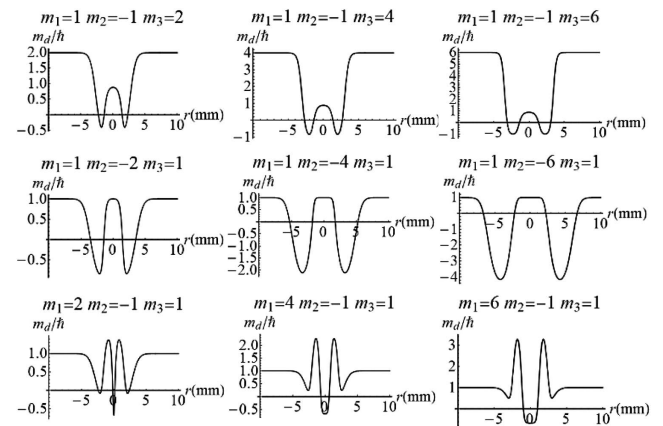


**Fig. 6.** Distributions of normalized OAM flux density  $m_d/h$  at  $z = 0$  with  $w_1 = 1$  mm,  $w_2 = 2$  mm,  $w_3 = 3$  mm,  $n_1 = n_2 = n_3 = 0$ , and  $\lambda_1 = \lambda_2 = \lambda_3 = 1$ .

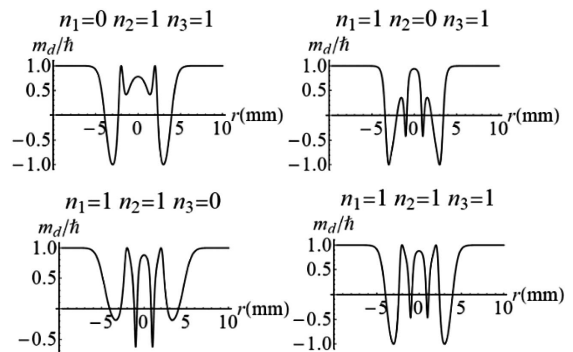


**Fig. 7.** Distributions of normalized OAM flux density  $m_d/h$  at  $z = 0$  with  $w_1 = 1$  mm,  $w_2 = 2$  mm,  $w_3 = 3$  mm,  $m_1 = +1$ ,  $m_2 = -1$ ,  $m_3 = 1$ , and  $\lambda_1 = \lambda_2 = \lambda_3 = 1$ .

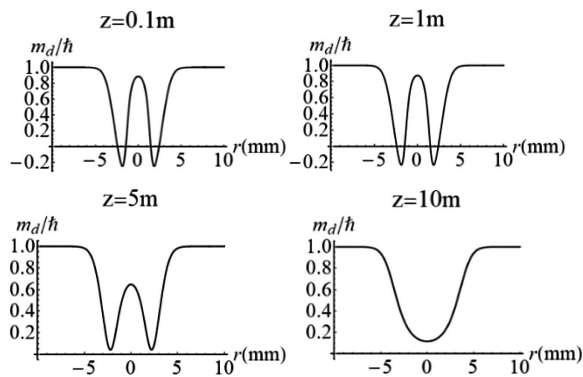


**Fig. 8.** Distributions of normalized OAM flux density  $m_d/h$  with  $w_1 = 1$  mm,  $w_2 = 2$  mm,  $w_3 = 3$  mm,  $m_1 = +1$ ,  $m_2 = -1$ ,  $m_3 = 1$ ,  $n_1 = n_2 = n_3 = 0$ ,  $\lambda_1 = \lambda_2 = 1$ , and  $\lambda = 632.8$  nm.

In all cases shown so far, the weights of the modes  $\lambda_n$  have been taken to be equal. We can also adjust the mode weights to emphasize one mode, and its OAM, over the others.

Finally, we note in Fig. 8 that, with three modes, the distribution of OAM changes significantly on propagation. In such a case, the OAM distribution being used to interact with a target could be modified by a simple change in propagation distance.

The results of this paper illustrate the great potential for using partial coherence to control the OAM of a beam, both in total and the distribution in a beam's cross-section. Even using two or three coherent modes, one gets a rich variety of counter-rotating regions along the radial direction. Changes in virtually any parameter in these simple beams can provide significant changes in the distribution of OAM. It is hoped that these results will provide an improved ability to control light-driven micromachines, and more sophisticated particle manipulation and rotation.

In concluding, it is important to note the difference between these incoherent superpositions of OAM modes and coherent superpositions. In a coherent superposition, interference effects will produce an azimuthally asymmetric beam, with bright and dark spots along the azimuthal direction. The partially coherent

OAM beams discussed here, however, have a uniform intensity and constant OAM density at any radial distance, making them much more suited for use in rotating objects.

**Funding.** National Natural Science Foundation of China (NSFC) (11474143, 91750201, 11525418); Air Force Office of Scientific Research (AFOSR) (FA9550-16-1-0240); Foundation of Henan Educational Committee (2016GGJS-116).

## REFERENCES

1. J. F. Nye and M. V. Berry, *Proc. R. Soc. Lond. A* **336**, 165 (1974).
2. M. S. Soskin and M. V. Vasnetsov, *Prog. Opt.* **42**, 219 (2001).
3. M. R. Dennis, K. O'Holleran, and M. J. Padgett, *Prog. Opt.* **53**, 293 (2009).
4. G. Gbur, *Singular Optics* (CRC Press, 2017).
5. L. Allen, M. W. Beijersbergen, R. J. C. Spreeuw, and J. P. Woerdman, *Phys. Rev. A* **45**, 8185 (1992).
6. D. G. Grier, *Nature* **424**, 810 (2003).
7. N. B. Simpson, K. Dholakia, L. Allen, and M. J. Padgett, *Opt. Lett.* **22**, 52 (1997).
8. G. Gibson, J. Courtial, M. J. Padgett, M. Vasnetsov, V. Pas'ko, S. M. Barnett, and S. Franke-Arnold, *Opt. Express* **12**, 5448 (2004).
9. J. C. Ricklin and F. M. Davidson, *J. Opt. Soc. Am. A* **19**, 1794 (2002).
10. C. Zhao, Y. Cai, X. Lu, and H. T. Eyyuboğlu, *Opt. Express* **17**, 1753 (2009).
11. J. Zhang, Z. Wang, B. Cheng, Q. Wang, B. Wu, X. Shen, L. Zheng, Y. Xu, and Q. Lin, *Phys. Rev. A* **88**, 023416 (2013).
12. H. F. Schouten, G. Gbur, T. D. Visser, and E. Wolf, *Opt. Lett.* **28**, 968 (2003).
13. G. Gbur and T. D. Visser, *Opt. Commun.* **222**, 117 (2003).
14. D. M. Palacios, I. D. Maleev, A. S. Marathay, and G. A. Swartzlander, Jr., *Phys. Rev. Lett.* **92**, 143905 (2004).
15. W. Wang and M. Takeda, *Phys. Rev. Lett.* **96**, 223904 (2006).
16. S. B. Raghunathan, H. F. Schouten, and T. D. Visser, *Opt. Lett.* **37**, 4179 (2012).
17. C. S. D. Stahl and G. Gbur, *Opt. Lett.* **39**, 5985 (2014).
18. J. Serna and J. M. Movilla, *Opt. Lett.* **26**, 405 (2001).
19. S. M. Kim and G. Gbur, *Phys. Rev. A* **86**, 043814 (2012).
20. Y. Cai and S. Zhu, *Opt. Lett.* **39**, 1968 (2014).
21. G. Gbur, *Proc. SPIE* **10549**, 1054903 (2018).
22. G. V. Bogatyryova, C. V. Fel'de, P. V. Polyanskii, S. A. Ponomarenko, M. S. Soskin, and E. Wolf, *Opt. Lett.* **28**, 878 (2003).
23. E. Wolf, *J. Opt. Soc. Am.* **72**, 343 (1982).